AMERICAN SOCIETY FOR MICROBIOLOGY | Journal of Virology

Influenza A Virus Dysregulates Host Histone Deacetylase 1 That Inhibits Viral Infection in Lung Epithelial Cells

Prashanth Thevkar Nagesh, Matloob Husain

Department of Microbiology and Immunology, University of Otago, Dunedin, New Zealand

ABSTRACT

Viruses dysregulate the host factors that inhibit virus infection. Here, we demonstrate that human enzyme, histone deacetylase 1 (HDAC1) is a new class of host factor that inhibits influenza A virus (IAV) infection, and IAV dysregulates HDAC1 to efficiently replicate in epithelial cells. A time-dependent decrease in HDAC1 polypeptide level was observed in IAV-infected cells, reducing to <50% by 24 h of infection. A further depletion (97%) of HDAC1 expression by RNA interference increased the IAV growth kinetics, increasing it by >3-fold by 24 h and by >6-fold by 48 h of infection. Conversely, overexpression of HDAC1 decreased the IAV infection by >2-fold. Likewise, a time-dependent decrease in HDAC1 activity, albeit with slightly different kinetics to HDAC1 polypeptide reduction, was observed in infected cells. Nevertheless, a further inhibition of deacetylase activity increased IAV infection in a dose-dependent manner. HDAC1 is an important host deacetylase and, in addition to its role as a transcription repressor, HDAC1 has been lately described as a coactivator of type I interferon response. Consistent with this property, we found that inhibition of deacetylase activity either decreased or abolished the phosphorylation of signal transducer and activator of transcription I (STAT1) and expression of interferon-stimulated genes, IFITM3, ISG15, and viperin in IAV-infected cells. Furthermore, the knockdown of HDAC1 expression in infected cells decreased viperin expression by 58% and, conversely, the overexpression of HDAC1 increased it by 55%, indicating that HDAC1 is a component of IAV-induced host type I interferon antiviral response.

IMPORTANCE

Influenza A virus (IAV) continues to significantly impact global public health by causing regular seasonal epidemics, occasional pandemics, and zoonotic outbreaks. IAV is among the successful human viral pathogens that has evolved various strategies to evade host defenses, prevent the development of a universal vaccine, and acquire antiviral drug resistance. A comprehensive knowledge of IAV-host interactions is needed to develop a novel and alternative anti-IAV strategy. Host produces a variety of factors that are able to fight IAV infection by employing various mechanisms. However, the full repertoire of anti-IAV host factors and their antiviral mechanisms has yet to be identified. We have identified here a new host factor, histone deacetylase 1 (HDAC1) that inhibits IAV infection. We demonstrate that HDAC1 is a component of host innate antiviral response against IAV, and IAV undermines HDAC1 to limit its role in antiviral response.

Influenza A virus (IAV), a prototypic member of family *Orthomyxoviridae*, has been a successful human respiratory pathogen. IAV has prevented the development of a universal vaccine so far and rendered the currently approved anti-influenza virus drugs almost ineffective. A unique genetic make-up comprising of a segmented RNA genome and a broad host range of humans, birds, pigs, dogs, cats, horses, seals, and bats allows the regular emergence of novel and drug-resistant IAV strains, causing regular seasonal epidemics, irregular pandemics, and zoonotic outbreaks (1, 2). The worldwide annual influenza vaccination program alternating in the northern and southern hemispheres is the major tool to prevent or control seasonal influenza epidemics. Despite this effort, according to the World Health Organization estimate, influenza manages to cause approximately 1 billion cases of flu, 3 to 5 million cases of severe illness, and 300,000 to 500,000 deaths worldwide annually (http://www.who.int/immunization/topics/influenza/en/). In addition, seasonal influenza epidemics result in significant productivity and economic losses due to work and school absenteeism, doctor visits, and hospitalizations. A new IAV pandemic further exacerbates these problems by many fold. Furthermore, frequent zoonotic outbreaks of deadly avian IAV infections in humans highlight the constant threat of the emergence of a new pandemic IAV strain (1, 2).

Therefore, there is a need to develop novel, alternative, and long-lasting anti-influenza strategies. One strategy is to strengthen host defenses by targeting the antiviral host factors. Host cells produce variety of factors that target various steps of virus life cycle to inhibit virus infection and multiplication (3). However, viruses have evolved their own strategies to antagonize those factors (3). Recently, we discovered that the human enzyme histone deacetylase 6 (HDAC6) has an anti-IAV function (4) and that IAV downregulates HDAC6 activity and induces a caspase-mediated cleavage of HDAC6 polypeptide to antagonize its antiviral function (5, 6). These findings led to the hypothesis that other human HDACs potentially have a similar role in IAV infection.

Received 20 January 2016 **Accepted** 16 February 2016

Accepted manuscript posted online 24 February 2016

Citation Nagesh PT, Husain M. 2016. Influenza A virus dysregulates host histone deacetylase 1 that inhibits viral infection in lung epithelial cells. J Virol 90:4614–4625. doi:10.1128/JVI.00126-16.

Editor: R. M. Sandri-Goldin

Address correspondence to Matloob Husain, matloob.husain@otago.ac.nz.

HDACs are a family of enzymes that catalyze the deacetylation of acetylated proteins (7). Acetylation is a posttranslational modification of proteins that has been discovered and studied extensively in histones to understand the chromatin structure and gene transcription (8, 9). Now, acetylation is also known to occur in a variety of nonhistone proteins. A proteomic study has identified at least 3,600 acetylation sites in 1,750 nuclear and nonnuclear proteins, indicating a broader role of acetylation/deacetylation in nuclear and cytoplasmic functions of the cell (10). Acetylation/deacetylation is a reversible process that is regulated by the competition of histone acetyltransferases (HATs) and HDACs, consequently influencing diverse cellular processes, such as the cell cycle, chromatin remodeling, RNA splicing, gene expression, cell signaling, and protein stability and transport (7, 11). HDACs are expressed in all eukaryotic cells. Mammalian HDACs are a family of at least 18 members, which have been classified into four classes based on their homology to yeast HDACs (12, 13). The class I, II, and IV HDACs are considered classical HDACs and are zinc dependent. The HDACs in each class vary in structure, enzymatic activity, intracellular localization, and expression pattern. The class I HDACs (HDAC1, -2, -3, and -8) are expressed in all tissues and are mainly localized to the nucleus. Class II HDACs, which are further subdivided into class IIa (HDAC4, -5, -7, and -9) and class IIb (HDAC6 and -10), shuttle between the nucleus and the cytoplasm (7, 12, 13). Class III HDACs, commonly known as sirtuins, comprise seven members (SIRT1 to -7). Each sirtuin has a unique subcellular localization and distinct function (14). The sirtuins are different than classical HDACs and require NAD^+ for enzymatic activity. Lastly, class IV has only one member, HDAC11, which shares homology with both class I and class II HDACs (12). Previously, we found that HDAC6, a class II HDAC, possesses an anti-IAV property and IAV undermines HDAC6 activity and integrity to limit its antiviral function (4–6). Likewise, we demonstrate here that HDAC1, a class I HDAC, also possesses anti-IAV properties and is an integral part of host type I interferon (IFN)-mediated response against IAV. In turn, IAV downregulates HDAC1 expression and deacetylase activity to antagonize its antiviral function and efficiently replicate in epithelial cells.

MATERIALS AND METHODS

Cells, viruses, and plasmids. A549 and MDCK cells were grown and maintained in complete minimum essential medium (MEM) supplemented with 10% fetal bovine serum (FBS), penicillin-streptomycin, and L-glutamine (Life Technologies) at 37°C and under 5% CO_2 atmosphere. Influenza virus A/PR/8/34 (H1N1) strain, A/New Caledonia/20/1999 (H1N1) strain, and A/WSN/34 (H1N1) strain (kindly provided by Richard Webby, St Jude Children's Research Hospital) were propagated in 10-day-old embryonated chicken eggs and titrated on MDCK cells. Human HDAC1 cloned in plasmid pcDNA3.1, a gift from Eric Verdin (Addgene plasmid 13820) (15) was prepared from *Escherichia coli* DH5α cells using a plasmid purification kit (Qiagen).

Infection. Cells were infected with IAV at a multiplicity of infection (MOI) of 0.1 to 5.0 PFU/cell. The virus inoculum was prepared in serum-free MEM and added to cell monolayers previously washed twice with serum-free MEM. For infection of MDCK cells, 1 μg of TPCK (tolylsulfonyl phenylalanyl chloromethyl ketone)-trypsin (Sigma-Aldrich)/ml was added to the virus inoculum. After 1 h of incubation at 35°C, the inoculum was removed and cells were washed once with serum-free MEM. Fresh serum-free MEM was added, and the cells were incubated back at 35°C. In some experiments, serum-free MEM was supplemented with NH_4Cl (Sigma-Aldrich), MG132 (Calbiochem), or trichostatin A (TSA; Sigma-Aldrich). To inactivate IAV, the virus inoculum was irradiated under a 30-W UV bulb for 5 min.

Quantitative real-time PCR of HDAC1. Total RNA from the cells was isolated by using a PureLink RNA isolation kit (Life Technologies). The integrity of isolated RNA was confirmed using RNA 6000 Nano Chip on Bioanalyzer 2100 (Agilent). The RNA purity (260/280 ratio of 2.0) and quantity were measured on a NanoDrop 1000 (Thermo). Total RNA was then used as a template to synthesize the cDNA using SuperScript III first-strand synthesis System (Life Technologies). The quantitative real-time PCR of HDAC1 was performed using SYBR green select master mix (Life Technologies) and KiCqStart primers (Sigma-Aldrich)—forward primer, 5′-GGATACGGAGATCCCTAATG-3′; reverse primer, 5′-CGT GTTCTGGTTAGTCATATTG-3′—on a ViiA 7 real-time PCR system (Applied Biosystems). Simultaneously, The beta-actin (forward primer, 5′-GACGACATGGAGAAAATCTG-3′; reverse primer, 5′-ATGATCTG GGTCATCTTCTC-3′) was amplified as a reference gene for normalization. The fold change in the expression of HDAC1 mRNA was calculated using the $2^{-\Delta\Delta CT}$ method as described elsewhere (16).

Western blotting. Cells were lysed in lysis buffer (50 mM Tris-HCl [pH 7.4], 150 mM NaCl, 0.5% sodium dodecyl sulfate [SDS], 0.5% sodium deoxycholate, 1% Triton X-100, and 1× protease inhibitor cocktail [Roche]). The total amount of protein was quantitated by using a BCA kit (Thermo). Equal amounts of proteins were resolved on 10 or 15% Tris-glycine SDS-PAGE under reducing conditions and transferred onto Protran Premium nitrocellulose membrane (GE Healthcare). Membranes were probed with mouse anti-HDAC1 (1:1,000; clone 10E2; Cell Signaling), rabbit anti-acetyl-histone H3 (Lys9; 1:1,000; clone C5B11; Cell Signaling), rabbit anti-histone H3 (1:1,000; clone D1H2; Cell Signaling), rabbit anti-IFITM3 (1:1,000; Abcam), rabbit anti-ISG15 (1:1,000; Cell Signaling), rabbit anti-viperin (1:1,000; clone D5T2X; Cell Signaling), mouse anti-STAT1 (1:1,000; clone 42/Stat1; BD Biosciences), mouse anti-STAT1 (pY701; 1:1,000; clone 14/P-STAT1; BD Biosciences), mouse anti-ubiquitin (1:500; clone P4D1; Santa Cruz), mouse anti-NP (1:1,000; NR-4282, obtained through BEI Resources, NIAID, NIH), goat anti-NP (1:1,000; kindly provided by Richard Webby), rabbit anti-actin (1:5,000; Abcam), or rabbit anti-protein disulfide isomerase (PDI; 1:5,000; Sigma-Aldrich) antibody, followed by horseradish peroxidase-conjugated anti-mouse, anti-goat, or anti-rabbit IgG antibody (1:5,000; Life Technologies). Protein bands were visualized by using a chemiluminescent substrate, and images were acquired on an Odyssey Fc imaging system (Li-Cor). Images were exported as TIFF files and compiled in Adobe Photoshop CC 2015.

HDAC activity assay. An *in situ* fluorometric HDAC activity kit (Sigma-Aldrich, catalog no. EPI003) was used to perform this assay. Briefly, cells grown in 96-well optical bottom plate (Nunc) were either mock infected or infected with IAV/PR/8/34 (H1N1) strain at an MOI of 0.5. After 20 h of infection, the cells were processed for the assay according to the manufacturer's protocol. The fluorescence excitation/emission was read at 368/442 nm on a Varioskan Flash fluorimeter (Thermo).

Overexpression of HDAC1. Cells were transfected with plasmids using Lipofectamine 2000 reagent (Life Technologies) by following the manufacturer's guidelines. Briefly, cells (4×10^5) were grown to 80–90% confluence in a 12-well culture plate (Corning). Plasmid DNA (1 μg) and Lipofectamine 2000 (3 μl) were diluted separately in Opti-MEM I medium (Life Technologies), mixed together, and incubated for 20 to 30 min at room temperature. The DNA-Lipofectamine 2000 complex was then added to the cells. The cells were grown at 37°C for 48 h before infection or further processing.

Knockdown of HDAC1 expression. Predesigned small interfering RNA (siRNA) oligonucleotides targeting the HDAC1 gene [CUGUACA UUGACAUUGAUA(dT)(dT)], and nontargeting Mission control siRNA was obtained from Sigma-Aldrich and delivered to the cells using Lipofectamine RNAiMax reagent (Life Technologies) according to the manufacturer's guidelines. Briefly, siRNA oligonucleotides (10 nM) and RNAiMax (2 μl) (Life Technologies) were diluted separately in Opti-

MEM I medium (Life Technologies), mixed together, and incubated for 20 to 30 min at room temperature. The siRNA-RNAiMax complex was then mixed with 2×10^5 cells and transferred to a 12-well culture plate. The cells were incubated at 37°C for 72 h before infection or further processing.

Cell viability assay. An MTT (3-[4,5-dimethylthiazol-2-yl]-2,5-diphenyl tetrazolium bromide) assay was performed to ascertain the viability of the cells. The MTT assay is based on the conversion of MTT into formazan crystals by living cells and determines the mitochondrial activity, which for most cell populations is related to the number of viable cells (17). Cells that had undergone various treatments were washed twice with phosphate-buffered saline. One milliliter of MTT reagent (Sigma-Aldrich) was added to the cells, and the cells were incubated at 37°C for 1 h. Subsequently, 1 ml of dimethyl sulfoxide (Calbiochem) was added, and the cells were further incubated for 15 to 20 min at room temperature, with shaking. Finally, the absorbance was measured at 595 nm on Multiskan Ascent plate reader (LabSystems).

Virus release assays. The culture medium from infected cells was harvested, the cell debris was cleared off by low-speed centrifugation, and the remainder was divided into two parts. One part was subjected to protein precipitation by trichloroacetic acid (TCA; Calbiochem), whereas the other part was mixed with 0.3% BSA and titrated on MDCK cells, followed by a microplaque assay. For protein precipitation, ice-cold TCA was mixed with culture medium at a final concentration of 20%, followed by incubation on ice for 30 min. The mixture was then centrifuged at 20,000 × *g* and 4°C for 30 min. The supernatant was removed carefully, and the pellet was washed twice with ice-cold acetone. The pellet was air dried and directly suspended in SDS-PAGE sample buffer (50 mM Tris-HCl [pH 6.8], 2% SDS, 30% glycerol, 5% 2-mercaptoethanol, and 0.04% bromophenol blue). Proteins were resolved by SDS-PAGE, and viral nucleoprotein (NP) was detected by Western blotting. For microplaque assay, confluent monolayers of MDCK cells were infected with 10-fold serial dilutions of the culture medium. The viral inoculum was removed, and the cells were overlaid with serum-free MEM containing 1 μg of TPCK-trypsin/ml and 0.8% Avicel (RC-581; FMC Biopolymer). After 18 to 20 h of incubation, the overlay was removed, and the cells were fixed with 4% formalin (Sigma-Aldrich) and subsequently permeabilized with 0.5% Triton X-100 in 200 mM glycine solution. The cells were then stained with mouse anti-NP antibody (1:1,000), followed by horseradish peroxidase-conjugated anti-mouse IgG antibody (1:1,000). Plaques were developed by adding a substrate solution containing AEC (3-amino-9-ethylcarbazole; Sigma-Aldrich) at 0.4 mg/ml in 0.05 M sodium acetate buffer (pH 5.5) and 0.03% hydrogen peroxide (Calbiochem).

Statistical analysis. All statistical analyses were performed using Prism 6 (GraphPad). The *P* values were calculated by using unpaired *t* tests for pairwise data comparisons, one-way analysis of variance (ANOVA), or two-way ANOVA for multiple data set comparisons. A *P* value of ≤0.05 was considered significant.

RESULTS

IAV downregulates the expression of HDAC1. We selected HDAC1 for the present study to test our hypothesis that like HDAC6, a class II HDAC, class I HDACs also possess anti-IAV properties. HDAC1 is a prototypic member of class I HDACs (13). It is well established that viruses subvert host cell transcription and translational machinery to express their own polypeptides and decrease or shut down the expression of host proteins involved in antiviral response (18, 19). Therefore, we first analyzed the expression of host HDAC1 in response to IAV infection. Human lung epithelial A549 cells were infected with influenza virus A/PR/8/34 (H1N1) strain (here referred as PR8) at an MOI of 0.5 PFU per cell, and the culture medium and the infected cells were harvested separately. The cells were processed to measure the level of HDAC1 mRNA by quantitative real-time PCR. We found that IAV infection caused a moderate 23% but statistically significant ($P = 0.005$) reduction in HDAC1 mRNA level in A549 cells (Fig. 1A). Similar results were obtained when cells were infected with PR8 at an MOI of 5.0 PFU per cell (data not shown). The infection of A549 cells was confirmed by detecting the presence of released IAV progeny in the culture media by plaque assay (data not shown).

After detecting a moderate, but statistically significant reduction in HDAC1 transcript level, we analyzed the level of HDAC1 polypeptide in A549 cells in response to IAV infection. Cells were infected with PR8 as above and harvested after 2, 6, 12, and 24 h of infection. The HDAC1 polypeptide was detected in total cell lysates by Western blotting (WB), and the intensities of protein bands were quantitated. We found that IAV infection reduced the level of HDAC1 polypeptide (62 kDa) in A549 cells in a time-dependent manner (Fig. 1B). There were significant 44% ($P = 0.015$), 63% ($P = 0.001$), and 67% ($P = 0.001$) decreases in HDAC1 polypeptide level after 6, 12, and 24 h of infection, respectively, compared to the 2-h postinfection time point (Fig. 1C). Further, there was a significant 57% ($P = 0.002$) decrease in HDAC1 polypeptide level after 24 h of infection compared to the uninfected cells harvested at the same time. A similar trend in HDAC1 polypeptide level reduction was observed when A549 cells were infected with PR8 at an MOI of 5.0 PFU per cell for 24 h (data not shown). Furthermore, the reduction in HDAC1 polypeptide level was even more profound and dose dependent when A549 cells were infected with IAV/WSN/33 (H1N1) strain for 24 h (Fig. 1D). Compared to the uninfected cells, approximately 80 and 95% decreases in the level of HDAC1 polypeptide were observed in cells infected with the WSN strain at MOIs of 3.0 and 5.0 PFU/cell, respectively (data not shown). Finally, by using a UV-irradiated PR8 inoculum, we confirmed that a replication-competent IAV was required to reduce the HDAC1 polypeptide levels in A549 cells (Fig. 1E). Furthermore, almost identical results were obtained when Fig. 1E experiment was repeated using the influenza virus A/New Caledonia/20/1999 (H1N1) strain, a more clinically relevant strain of IAV (Fig. 1F).

The lack of a linear correlation between the reduction of HDAC1 mRNA and polypeptide levels in PR8-infected cells prompted us to investigate whether IAV promotes the degradation of HDAC1 polypeptide in infected cells. Two main pathways, one mediated by proteasome and other mediated by lysosome, govern the degradation of proteins in eukaryotic cells. To identify the pathway leading to the degradation of HDAC1 polypeptide in IAV-infected cells, PR8-infected cells were treated with proteasome inhibitor MG132 (20 μM) or lysosome inhibitor NH_4Cl (20 mM); at these concentrations, MG132 and NH_4Cl have been shown to inhibit proteasomal and lysosomal activity, respectively (20, 21). The levels of HDAC1 polypeptide were then analyzed and quantified as described above. We found that MG132 treatment reversed the effect of IAV infection on HDAC1 polypeptide level and rescued its level in infected cells almost to the level of uninfected cells, whereas NH_4Cl treatment did not reverse the effect of IAV infection on HDAC1 polypeptide level (Fig. 1G). Consistent with above data, there was a significant 54% ($P = 0.001$) and 60% ($P = 0.0004$) decrease in HDAC1 polypeptide level in mock-treated and NH_4Cl-treated infected cells, respectively, compared to their uninfected controls (Fig. 1H). In contrast, there was an insignificant 3% decrease in HDAC1 polypeptide level in MG132-treated infected cells compared to the uninfected con-

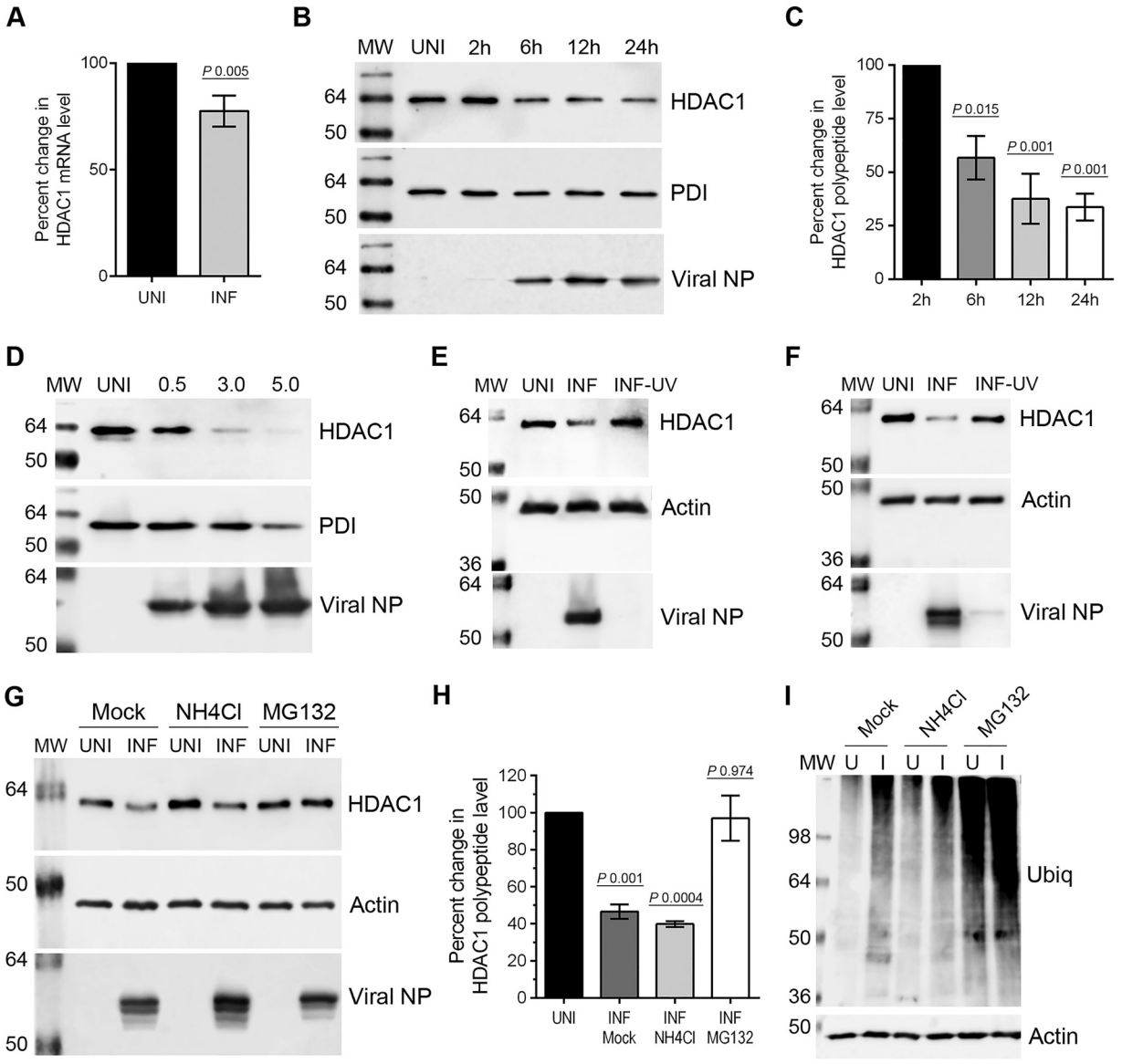

FIG 1 IAV downregulates the expression of HDAC1. (A) A549 cells (8×10^5) were infected with PR8 at an MOI of 0.5 for 24 h. The uninfected (UNI) and infected (INF) cells were harvested and processed, and HDAC1 mRNAs and beta-actin mRNAs were detected by quantitative real-time PCR. The level of HDAC1 mRNA was normalized to beta-actin mRNA. The normalized value of HDAC1 mRNA in UNI sample was considered 100% for comparison to the INF sample. Error bars represents the means ± the standard errors of the means of three independent experiments; the *P* value was calculated using a *t* test. (B) A549 cells were infected as described above and harvested at the indicated times. Total cell lysates were prepared, and HDAC1 (62 kDa), PDI (57 kDa), and viral NP (56 kDa) were detected in uninfected and infected (2, 6, 12, and 24 h) cell lysates by WB. PDI was detected as the loading control, and NP was detected as the infection marker. (C) The HDAC1 and PDI protein bands were quantified using Image Studio Lite V4.0 software (Li-Cor), and the amount of HDAC1 was normalized to PDI. The normalized amount of HDAC1 in the UNI sample or the 2-h sample was considered 100% for comparisons to the 6-, 12-, and 24-h samples. Data presented are means ± the standard errors of the means of three independent experiments; the *P* value was calculated using one-way ANOVA. (D) A549 cells were infected with IAV WSN strain at an MOI of 0.5, 3.0 and 5.0 for 24 h. Total cell lysates were prepared, and HDAC1, PDI, and NP were detected in UNI and infected (0.5, 3.0, and 5.0) cell lysates by WB. (E) A549 cells were infected with live or UV-irradiated PR8 at an MOI of 0.5 for 24 h. Total cell lysates were prepared, and HDAC1, actin (42 kDa, as loading control), and NP were detected in UNI, INF, and INF-UV cell lysates by WB. (F) A549 cells were infected with live or UV-irradiated influenza virus A/New Caledonia/20/1999 (H1N1) strain at an MOI of 0.5 for 24 h. Total cell lysates were prepared, and HDAC1, actin, and NP were detected in UNI, INF, and INF-UV cell lysates by WB. (G) A549 cells were infected with PR8 as described above and subsequently treated with NH_4Cl (20 mM) or MG132 (10 μM) for 24 h. Total cell lysates were prepared, and HDAC1, actin, and NP were detected in UNI and INF cell lysates by WB. (H) The HDAC1 and actin protein bands were quantified as described above, and the amount of HDAC1 was normalized to actin. The normalized amount of HDAC1 in respective UNI samples was considered 100% for comparisons to INF samples. The data presented are means ± the standard errors of the means of three independent experiments; the *P* value was calculated by using one-way ANOVA. (I) Ubiquitin (Ubiq) and actin were detected in the cell lysates described above by WB. U, uninfected; I, infected. MW, molecular weight.

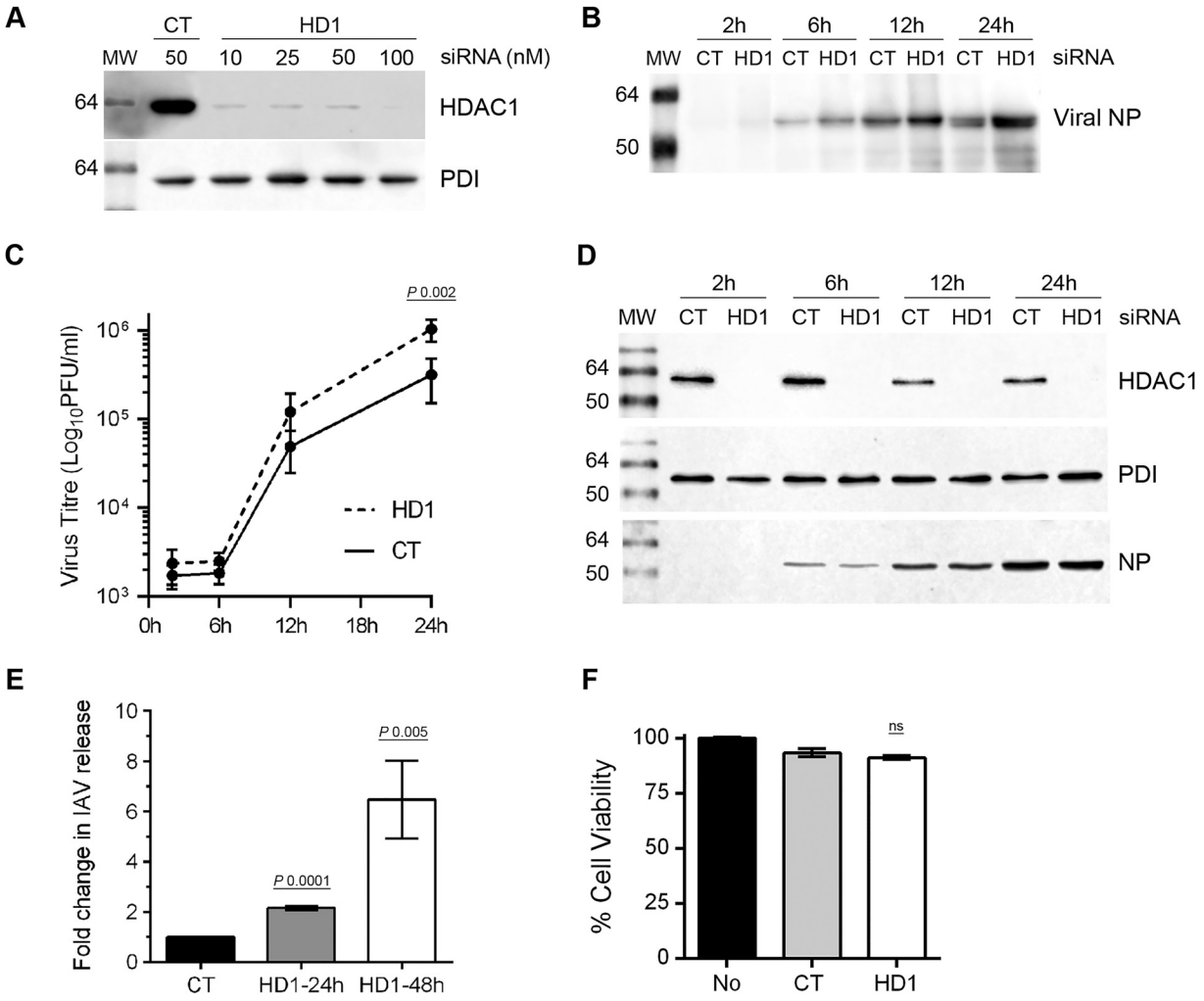

FIG 2 The knockdown of HDAC1 expression promotes IAV infection. (A) A549 cells (2×10^5) were transfected with indicated concentrations of nontargeting control (CT) siRNA or HDAC1-targeting (HD1) siRNA for 72 h. Total cell lysates were prepared, and HDAC1 and PDI were detected by WB. (B to D) A549 cells were transfected with 10 nM CT siRNA or HD1 siRNA for 72 h. The cells were then infected with PR8 at an MOI of 0.5, and the culture medium and the cells were harvested separately after 2, 6, 12, and 24 h of infection. The virion yield in the culture medium was measured by WB of NP (B) and by microplaque assay (C). The data presented are means ± the standard errors of the means of three independent experiments; the *P* value was calculated by using two-way ANOVA. (D) Total lysates of the cells were prepared, and HDAC1, PDI, and NP were detected by WB. (E) A549 cells transfected with CT or HD1 siRNAs, as described above, were infected with PR8 at an MOI of 0.1 in the presence of 0.1 μg of trypsin/ml, and the virion yield in the culture medium was measured by microplaque assay after 24 and 48 h. The virion yield from respective CT siRNA samples was considered to be 1-fold for comparisons to HD1 siRNA samples. The data presented are means ± the standard errors of the means of three independent experiments; the *P* values were calculated using one-way ANOVA. (F) A549 cells were transfected with no siRNA, CT siRNA, or HD1 siRNA for 72 h. The cell viability was determined using an MTT assay. MW, molecular weight; ns, not significant.

trol (Fig. 1H), indicating that IAV promoted the degradation of HDAC1 polypeptide by the proteasome pathway. An increase in the amount of ubiquitinated proteins in MG132-treated cells confirmed the potency of MG132 (Fig. 1I).

Endogenous HDAC1 possesses an anti-IAV property. The downregulation of HDAC1 expression in infected cells indicated a potential anti-IAV function for HDAC1. To test this, we analyzed the growth kinetics of IAV in A549 cells depleted of HDAC1 expression by RNA interference. First, various concentrations of a human HDAC1-targeting siRNA (10 to 100 nM) and a nontargeting control siRNA (50 nM) were delivered to A549 cells to obtain a significant depletion of HDAC1 expression. A 10 nM siRNA concentration was sufficient to knock down HDAC1 expression by 97% in A549 cells (Fig. 2A), with negligible cytotoxicity compared to control siRNA (Fig. 2F). Therefore, in the next and subsequent experiments, A549 cells were transfected with 10 nM HDAC1-targeting siRNA, as well as nontargeting control siRNA. The cells were then infected with PR8 (MOI of 0.5), and the culture medium and the infected cells were harvested separately after 2, 6, 12, and 24 h of infection. The culture medium was divided into two parts; one part was analyzed by WB, and the other part was titrated by plaque assay to measure the amount of total and infectious IAV progeny released, respectively. The lysates of infected cells were subjected to WB to confirm the depletion of HDAC1 expression. We found that IAV exhibits a higher growth characteristic in HDAC1-depleted cells (Fig. 2). After 12 and 24 h of infection, the cells transfected with HDAC1-targeting siRNA released more total virions than the cells transfected with control

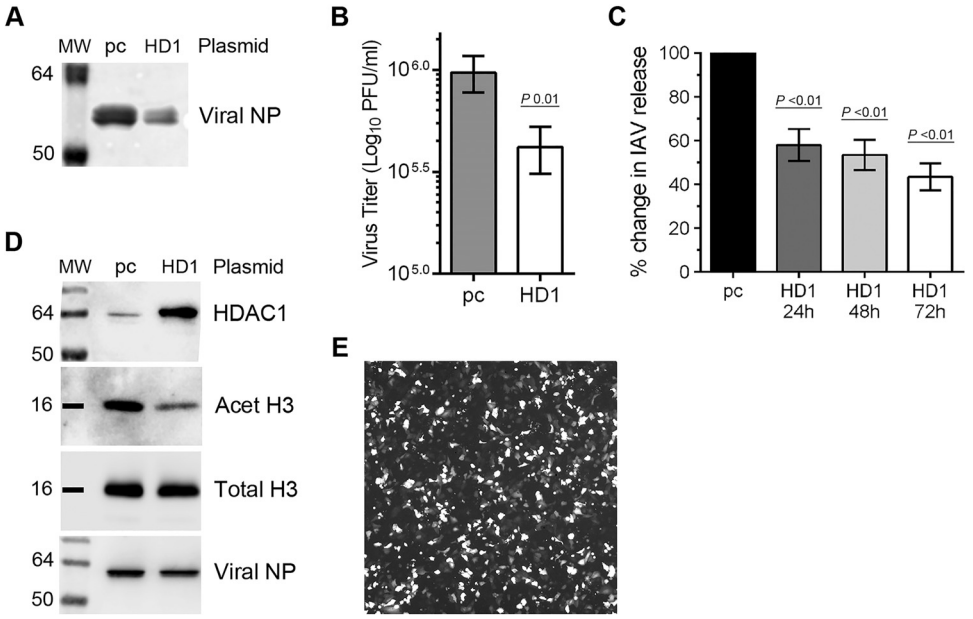

FIG 3 The overexpression of HDAC1 inhibits IAV infection. (A, B, and D) A549 cells (8×10^5) were transfected with empty plasmid pcDNA3 (pc) or pcDNA3 containing HDAC1 (HD1) for 48 h. Cells were then infected with PR8 at an MOI of 0.5, and the culture medium and the cells were harvested separately after 24 h. The virion yield in the culture medium was measured by WB of NP (A) and by microplaque assay (B). The data presented are means ± standard errors of the means of three independent experiments; the *P* value was calculated using a *t* test. (C) A549 cells transfected with pc or HD1 plasmids, as described above, were infected with PR8 at an MOI of 0.1 in the presence of 0.1 μg of trypsin/ml, and the virion yield in the culture medium was measured by microplaque assay after 24, 48, and 72 h. The virion yield from "pc" samples was considered 100% for comparisons to HD1 samples. The data presented are means ± the standard errors of the means of three independent experiments; the *P* value was calculated by using one-way ANOVA. (D) Total lysates of the cells were prepared, and HDAC1, acetylated-histone H3 (Lys9) (Acet H3; 17 kDa), total histone H3 (Total H3, 17 kDa), and NP were detected by WB. Acet H3 was detected as the HDAC1 substrate, and total H3 was detected as the loading control. (E) Transfection efficiency of A549 cells. Cells were transfected with a plasmid expressing green fluorescent protein as above. The cells were viewed, and an image was acquired on an inverted fluorescence microscope (Olympus) under a magnification of ×10. MW, molecular weight.

siRNA (Fig. 2B). Similarly, cells transfected with HDAC1-targeting siRNA released 2.4- and 3.2-fold ($P = 0.002$) more infectious virions after 12 and 24 h of infection, respectively, than the cells transfected with control siRNA at the corresponding times (Fig. 2C). The WB analysis of infected cell lysates confirmed the depletion of HDAC1 expression at each time point (Fig. 2D). Immunofluorescent staining of NP, followed by confocal microscopy, was used to ascertain that a similar percentage of HDAC1-targeting siRNA (92.4 ± 1.2, $n = 5$)- and control siRNA (93.2 ± 2.2, $n = 5$)-transfected cells were infected with PR8 after 12 h. Likewise, when infected with PR8 at an MOI of 5.0, HDAC1-depleted A549 cells released 2.3-fold more infectious virions than the control cells after 24 h (data not shown). To further substantiate the higher IAV growth kinetics in the absence of endogenous HDAC1, HDAC1-depleted cells were infected with PR8 at an MOI of 0.1 in the presence of trypsin, and the release of infectious IAV progeny was measured after 24 and 48 h, as described above. Consistent with above data, cells transfected with HDAC1-targeting siRNA released a 2.15-fold ($P = 0.0001$) more infectious virions than the cells transfected with control siRNA after 24 h of infection (Fig. 2E). After the 48 h of infection, the release of infectious IAV progeny from HDAC1-depleted cells was further increased to 6.4-fold ($P = 0.005$) compared to control cells (Fig. 2E). Similarly, when infected with PR8 at an MOI of 0.01 in the presence of trypsin, cells transfected with HDAC1-targeting siRNA released 1.6- and 6.8-fold more infectious virions than did the cells transfected with control siRNA after 24 and 48 h of infection, respectively (not shown).

Ectopically expressed HDAC1 inhibits IAV infection. The data presented above demonstrated that endogenously expressed HDAC1 has an anti-IAV property and that IAV grows to a higher titer in HDAC1-depleted A549 cells. Next, we wanted to find out whether ectopically expressed HDAC1 would have the opposite effect. A549 cells were transfected with an HDAC1-expressing plasmid or an empty plasmid and subsequently infected with PR8 at an MOI of 0.5 for 24 h. The culture medium and the infected cells were harvested separately. The culture medium was analyzed by WB and plaque assay as in Fig. 2B and C, respectively. The cell lysates were subjected to WB to analyze the HDAC1 overexpression and subsequent effect of overexpressing HDAC1 on its substrate acetylated-histone H3 (Lys9) (22–25). Indeed, in contrast to the results obtained with HDAC1 depletion, the overexpression of HDAC1 caused a reduction in IAV infection (Fig. 3). The HDAC1-overexpressing cells released less total viral progeny (Fig. 3A) and a significant 2.3-fold ($P = 0.01$) fewer infectious virions (Fig. 3B) in the culture medium than did the cells transfected with empty plasmid. Likewise, when infected with PR8 at an MOI of 0.1 in the presence of trypsin, the HDAC1-overexpressing cells released 42% ($P < 0.01$), 47% ($P < 0.01$), and 57% ($P < 0.01$) less infectious viral progeny after 24, 48, and 72 h of infection, respectively, than did the cells transfected with empty plasmid (Fig. 3C). Similar results were obtained when cells were infected with PR8 at an MOI of 5.0 for 24 h (data not shown). The overexpression of HDAC1 in cells was confirmed by WB (Fig. 3D). A visually noticeable reduction in the acetylated-histone H3 (Lys9) level and a negligible change in total histone H3 level in HDAC1-overex-

pressing cells compared to empty plasmid control confirmed that the ectopically expressed HDAC1 was enzymatically active (Fig. 3D). A fluorescence microscopy image showing the transfection efficiency of A549 cells is shown in Fig. 3E; a transfection efficiency of 60 to 70% was achieved routinely.

IAV downregulates HDAC1 activity. After discovering that HDAC1 polypeptide has an anti-IAV property and IAV downregulates its expression to potentially undermine its antiviral function, we next examined whether HDAC1 enzymatic activity is also downregulated in infected cells. To assess this, we compared the levels of HDAC1 substrate, acetylated-histone H3 in infected cell lysates with uninfected cell lysates by WB. An increase in acetylated-histone H3 level would mean that HDAC1 activity is downregulated and vice versa. To detect acetylated-histone H3, we selected an antibody (C5B11; Cell Signaling) that detects acetylated-histone H3 (Lys9), i.e., histone H3 acetylated on lysine residue at position 9. Previously, acetylated-histone H3 (Lys9) has been shown to be a specific substrate for HDAC1 (24, 25), and our HDAC1 overexpression data presented above (Fig. 3D) have confirmed it as an HDAC1 substrate. A time course experiment revealed that IAV downregulates the HDAC1 activity, and it does this mainly between 6 and 12 h of infection (Fig. 4A), which is the growth period of IAV in cultured cells (Fig. 2C). There were significant 3.0-fold ($P = 0.02$) and 3.38-fold ($P = 0.009$) increases in the levels of acetylated-histone H3 (Lys9) in infected cells after 6 and 12 h of infection, respectively, compared to uninfected cells (Fig. 4B). Interestingly, after 24 h of infection, the HDAC1 activity in infected cells (1.74-fold) came back up almost to the level of uninfected cells (Fig. 4B).

The deacetylase activity of class I and class II HDACs has anti-IAV properties. The downregulation of HDAC1 activity by IAV indicated an anti-IAV role for HDAC1 activity. One way to further investigate this is by using a selective inhibitor of HDAC1 enzymatic activity. However, to our knowledge, a selective HDAC1 inhibitor is not commercially available; most of the available HDAC inhibitors cross-inhibit other class I and class II HDACs (26). So, we determined the combined activity of class I and II HDACs (12) in response to IAV infection. To accomplish this, we used an *in situ* fluorometric HDAC activity assay kit, which essentially measures the activity of class I and class II HDACs. This kit utilizes a cell-permeable HDAC substrate containing an acetylated lysine side chain, which is deacetylated by intracellular HDACs. A developer then cleaves the deacetylated substrate and releases a fluorophore, which can be quantified. Using this kit, we measured an ~35% reduction in HDAC activity in infected cells compared to uninfected cells (not shown). Next, we sought to determine whether class I and class II HDAC activity has an anti-IAV function. To accomplish this, we used trichostatin A (TSA), an antifungal antibiotic that is widely used as an inhibitor of class I and class II HDACs, including HDAC1 (27). We found that, like HDAC1 depletion, TSA treatment increased the release of infectious IAV progeny and in a dose-dependent manner (Fig. 5). Compared to mock-treated infected cells, treatment of infected cells with 1 and 5 μM TSA resulted in significant 3.1-fold ($P = 0.03$) and 5.3-fold ($P = 0.001$) increases, respectively, in the release of infectious IAV progeny (Fig. 5A) and a negligible effect on infected cell viability (Fig. 5B). A corresponding increase in the levels of acetylated-histone H3 (Lys9), but not total histone H3 in TSA-treated cells indicated the inhibition of class I (including HDAC1) and class II HDAC activity (Fig. 5C).

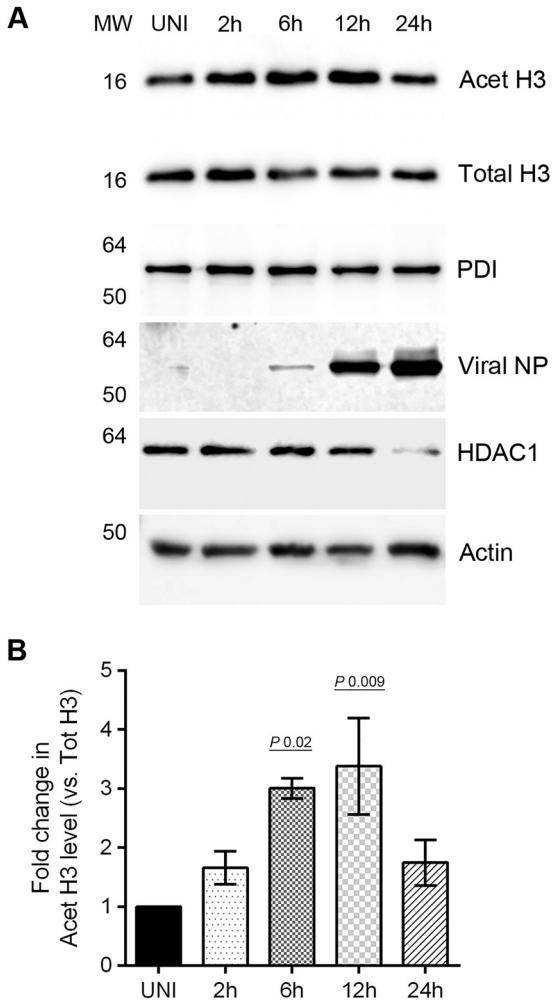

FIG 4 IAV downregulates the activity of HDAC1. (A) MDCK cells (8×10^5) were infected with PR8 at an MOI of 0.5 and harvested after 2, 6, 12, and 24 h of infection. Total cell lysates were prepared, and acetylated-histone H3 (Lys9) (Acet H3), total histone H3 (Total H3), PDI, HDAC1, actin, and NP were detected in uninfected (UNI) and infected (2, 6, 12, and 24 h) cell lysates by WB. Acet H3, an HDAC1 substrate, was detected as a marker of HDAC1 activity, and total H3, PDI, and actin were detected as loading controls. (B) Acet H3 and total H3 protein bands were quantified as Fig. 1C, and the amount of Acet H3 was normalized to the total H3. The normalized amount of Acet H3 in UNI sample was considered 1-fold for comparisons to 2-, 6-, 12-, and 24-h samples. The data presented are means ± the standard errors of the means of three independent experiments; the *P* value was calculated by using one-way ANOVA. MW, molecular weight.

The deacetylase activity of class I and class II HDACs is important for IAV-induced host type I IFN-mediated response. An increase in the release of infectious IAV progeny from TSA-treated cells confirmed that the enzymatic activity of class I and class II HDACs has anti-IAV properties. We next endeavored to determine the anti-IAV mechanism of class I and class II HDAC activity. In addition to its role in host gene transcription, the deacetylase activity of class I and class II HDACs has been shown to be a coactivator of type I interferon (IFN)-mediated host innate antiviral response and the subsequent expression of IFN-stimulated genes (ISGs) (28–32). However, a precise role of class I and class II HDACs in IAV-induced host innate antiviral response is yet to be

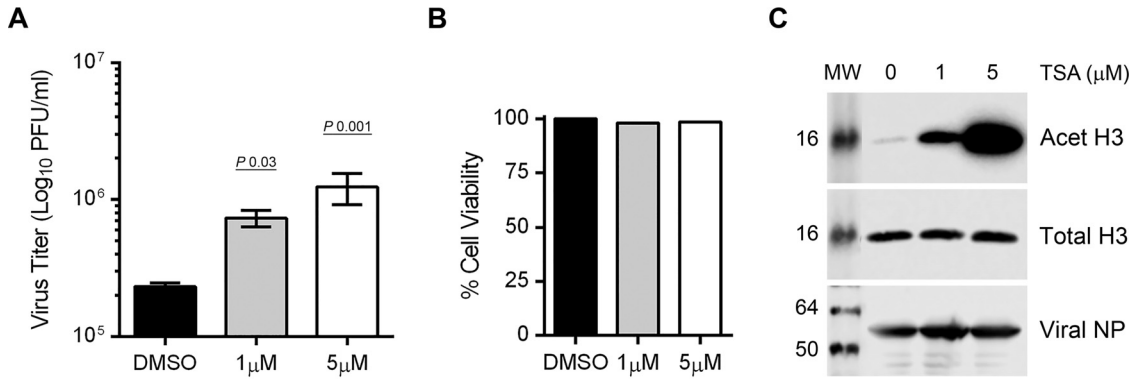

FIG 5 The inhibition of HDAC activity promotes IAV infection. (A to C) A549 cells (8×10^5) were infected with PR8 at an MOI of 0.5 and subsequently treated with dimethyl sulfoxide (DMSO) or the indicated concentrations of TSA (in DMSO) for 24 h. (A) The culture medium and the cells were harvested separately, and the virion yield in the culture medium was measured by microplaque assay. The data presented are means ± the standard errors of the means of three independent experiments; the *P* value was calculated by using one-way ANOVA. (B) A549 cells were infected and treated with DMSO and TSA for 24 h, and the cell viability was determined by an MTT assay. The viability of DMSO-treated infected cells was considered 100% for comparison to TSA-treated infected cells. (C) Total cell lysates were prepared, and Acet H3, total H3, and NP were detected by WB as the markers of TSA potency, loading control, and infection, respectively. MW, molecular weight.

understood. It has been well established that host cells produce type I IFNs upon IAV infection (33). Type I IFNs then engage host cell type I IFN receptor in an autocrine and paracrine manner and activate the cytoplasmic Janus kinases (JAKs) that in turn, phosphorylate the cytoplasmic signal transducer and activator of transcription 1 (STAT1). The phosphorylated STAT1 (pSTAT1) then translocates to the nucleus and forms a transcription complex called ISG factor 3 (ISGF3). ISFG3 then binds to the IFN-stimulated response element of ISGs in a sequence-specific manner and induces the expression of over 300 ISGs, including IFITM3, ISG15, and viperin, which inhibit IAV infection by targeting various steps of the virus life cycle (33–36). To induce the expression of ISGs, ISGF3 specifically interacts with several coactivators, which include class I and class II HDACs, particularly HDAC1 (28–32). Therefore, to determine the role of class I and class II HDAC activity in type I IFN-mediated host response against IAV, we treated the PR8-infected cells with TSA (1 and 5 μM) and analyzed the levels of pSTAT1 and ISGs, i.e., IFITM3, ISG15, and viperin, by WB. A decrease in the levels of these proteins in TSA-treated infected cells compared to untreated infected cells would indicate the involvement of class I and class II HDAC activity in type I IFN-mediated host antiviral response against IAV. As expected, IAV infection induced the phosphorylation of STAT1 and expression of IFITM3, ISG15, and viperin in A549 cells (Fig. 6). Consistent with this hypothesis, TSA treatment reduced the level of pSTAT1 (Fig. 6A), as well as the levels of IFITM3 (Fig. 6B), ISG15 (Fig. 6C), and viperin (Fig. 6D), in infected cells. TSA seems to have a dose-dependent effect on the phosphorylation of STAT1 (Fig. 6A) and the expression of ISG15 (Fig. 6C), whereas it has more profound effect on the expression of IFITM3 (Fig. 6B) and viperin (Fig. 6D), since they were barely detectable in infected cells treated with TSA.

HDAC1 is involved in IAV-induced viperin expression. It has been demonstrated that HDAC1 specifically coactivates the promyelocytic leukemia zinc finger and promyelocytic leukemia proteins that are involved in type I IFN-mediated innate immune response and subsequent expression of ISGs like viperin (32, 37). The above data demonstrated that class I and class II HDAC activity is required for the IAV-induced host type I IFN-mediated antiviral response and the expression of ISGs, including viperin. Therefore, we next sought to determine whether HDAC1 plays a specific role in the expression of viperin in IAV-infected cells. To accomplish this, HDAC1 expression was either depleted by RNA interference (as in Fig. 2) or increased from a plasmid (as in Fig. 3) in A549 cells before infecting them with PR8 and subsequently measuring the viperin levels by WB (as in Fig. 6D). Consistent with the data presented in Fig. 6, viperin expression was decreased in HDAC1-depleted infected cells (Fig. 7A) and increased in HDAC1-overexpressing infected cells (Fig. 7C). About 58% less ($P = 0.0001$) viperin was detected in infected cells transfected with HDAC1-targeting siRNA than in infected cells transfected with nontargeting control siRNA (Fig. 7B). Conversely, about 55% more ($P = 0.0001$) viperin was detected in infected cells transfected with HDAC1-expressing plasmid than in infected cells transfected with empty plasmid (Fig. 7D). Interestingly, a noticeable increase in the basal level of viperin was also observed in uninfected cells transfected with HDAC1-expressing plasmid (Fig. 7C).

DISCUSSION

The data presented here demonstrate that HDAC1 is a component of host antiviral response against IAV and that, in turn, IAV dysregulates HDAC1 to undermine its role in host antiviral response. IAV downregulates HDAC1 expression at both the mRNA and the polypeptide level. The reduction in HDAC1 mRNA level in IAV-infected cells observed here is consistent with a recent microarray-based gene expression profiling study (38). By using mainly a luciferase reporter assay and quantitative real-time PCR, Buggele et al. (38) demonstrated that IAV induces host microRNA, miR-449b that targets the 3′ untranslated region of HDAC1 mRNA, and when added exogenously, miR-449b further reduced HDAC1 mRNA level in infected cells. However, they did not determine HDAC1 polypeptide level in response to the direct IAV infection and could not establish a direct anti-IAV role of miR-449b or HDAC1 since the depletion or overexpression of miR-449b did not have an effect on IAV infection (38). Here, we demonstrated that IAV also reduces the HDAC1 polypeptide level in infected cells by promoting its degradation by a proteasomal pathway. A

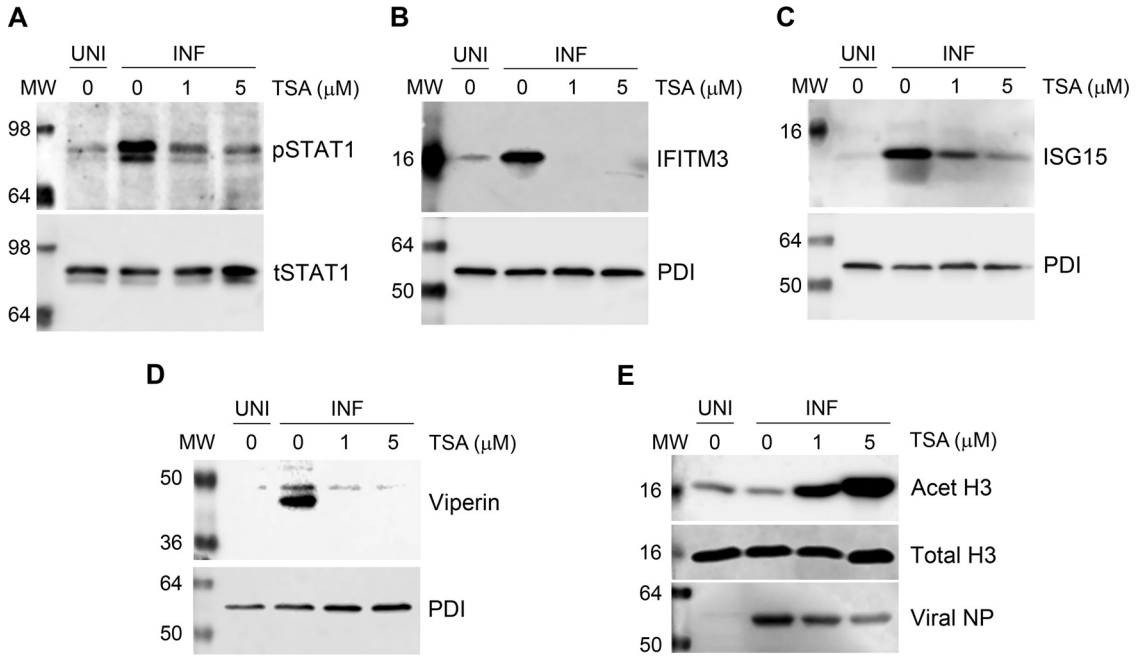

FIG 6 The inhibition of HDAC activity inhibits the phosphorylation of STAT1 and expression of ISGs. (A to E) A549 cells (8×10^5) were infected with PR8 at an MOI of 0.5 and subsequently treated with DMSO or the indicated concentrations of TSA (in DMSO) for 24 h. Total cell lysates were prepared, and phosphorylated STAT1 (pSTAT1, 91/84 kDa), along with total STAT1 (tSTAT1) as a loading control (A), and IFITM3 (15 kDa) (B), ISG15 (15 kDa) (C), or viperin (42 kDa) (D), along with PDI as loading control, were detected in uninfected (UNI) and infected (INF) cell lysates by WB. (E) In the same lysates, Acet H3, total H3, and NP were detected by WB as the markers of TSA potency, loading control, and infection, respectively. MW, molecular weight.

proteasome-mediated degradation of HDAC1 polypeptide is plausible, because HDAC1 has been previously reported to be ubiquitinated by Mdm2 E3 ubiquitin ligase (39, 40). It remains to be determined whether HDAC1 is also ubiquitinated in IAV-infected cells. A previous study reported an increase in IAV entry in HDAC1-depleted cells using a microscopy-based assay, but it did not monitor productive IAV replication cycles measuring the release of IAV progeny from HDAC1-depleted cells and did not envisage an anti-IAV role for HDAC1 (41). The outcomes of the HDAC1 knockdown and overexpression experiments described here showing an increase and decrease in IAV progeny release, respectively, confirmed an anti-IAV role of host HDAC1. However, such increase or decrease did not result in a noticeable increase or decrease in intracellular NP levels in HDAC1-depleted or HDAC1-overexpressing cells, respectively. A plausible explanation for this is that NP is one of the most abundant IAV proteins in infected cells, and a significant, but modest 2- to 3-fold difference in IAV infection may only slightly alter the intracellular abundance of NP in HDAC1-depleted or HDAC1-overexpressing cells, which may not be discernible by WB. Further, a significant, but modest 3-fold increase in the growth characteristics of IAV in HDAC1-depleted cells after 24 h could be partly attributed to the compensatory role of other class I HDACs in the absence of HDAC1. HDAC1 shares at least 86% similarity in nucleotide sequence with HDAC2 and about 63% similarity with HDAC3 (13, 25). It is believed that HDAC1 and HDAC2 genes are a duplicated copy of one gene derived from a common ancestor (13). Evidently, depletion of HDAC1 expression results in the enhanced expression of HDAC2 and HDAC3 (23, 25; P. T. Nagesh and M. Husain, unpublished data). A further investigation is under way to determine the role of HDAC2 and HDAC3 alone, as well as in conjunction with HDAC1 in IAV infection.

The data showed that deacetylase activity also has an anti-IAV function. Therefore, in addition to expression, IAV also downregulated the deacetylase activity of HDAC1, as determined by detecting the increase in the levels of specific HDAC1 substrate, acetylated-histone H3 (Lys9) (24, 25) in infected cells. One could argue that the increase in the levels of acetylated-histone H3 (Lys9) in IAV-infected cells is due to the decrease in the levels of HDAC1 polypeptide. However, time course experiments revealed a slightly different kinetics for decrease in the HDAC1 polypeptide levels and increase in the acetylated-histone H3 (Lys9) levels. For instance, HDAC1 polypeptide level continued to decrease after 12 h of infection, whereas the HDAC1 deacetylase activity started to come back up to the basal level after 12 h of infection. Nevertheless, a further investigation is needed to delineate the independent roles of HDAC1 catalytic domain and the rest of the HDAC1 polypeptide in its anti-IAV function.

The HDAC1, a mammalian homolog of the yeast pleiotropic transcriptional regulator Rpd3, was the first protein to be shown to have deacetylase activity (42). HDAC1 is primarily localized to the nucleus and prominently deacetylates acetylated lysine residues present at the N-terminal tails of histone H3 and H4 (25). Further, HDAC1 is believed to be the main driver of overall cellular deacetylase activity (23). The catalytic activity of HDAC1 (and HDAC2) is largely dependent on its association with multiprotein complexes, which include Sin3, NuRD, CoREST, and NODE complexes (13). It remains to be investigated whether IAV destabilizes or prevents the formation of these complexes to downregulate the HDAC1 activity. Historically, HDAC1 has been described

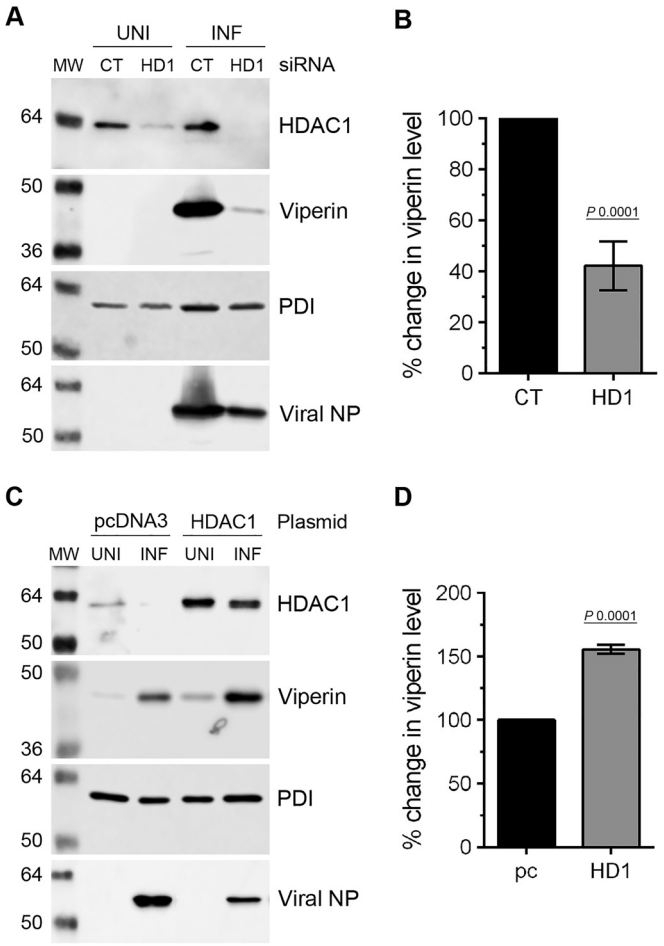

FIG 7 HDAC1 is involved in the expression of viperin in IAV-infected cells. (A and B) The knockdown of HDAC1 expression decreased viperin expression in infected cells. A549 cells (2×10^5) were transfected with nontargeting control (CT) siRNA or HDAC1-targeting (HD1) siRNA for 72 h. The cells were then infected with PR8 at an MOI of 0.5 for 24 h. (A) Total cell lysates were prepared, and HDAC1, viperin, PDI, and NP were detected in uninfected (UNI) and infected (INF) cell lysates by WB. (B) The viperin and PDI protein bands were quantified as Fig. 1C, and the amount of viperin was normalized to PDI. The normalized amount of viperin in CT siRNA-transfected INF cells was considered 100% for comparisons to HD1 siRNA-transfected INF cells. The data presented are means ± the standard errors of the means of three independent experiments; the *P* value was calculated using a *t* test. (C and D) The overexpression of HDAC1 increased viperin expression in infected cells. A549 cells (8×10^5) were transfected with empty plasmid pcDNA3 or pcDNA3 containing HDAC1 for 48 h. The cells were then infected with PR8 at an MOI of 0.5 for 24 h. (C) Total cell lysates were prepared, and HDAC1, viperin, PDI, and NP were detected in uninfected (UNI) and infected (INF) cell lysates by WB. Lanes 1 to 3 were combined with lanes 4 and 5 of the same blot to remove an unwanted lane from the middle. (D) The percent change in viperin level was calculated as described above. The data presented are means ± the standard errors of the means of three independent experiments; the *P* value was calculated using a *t* test. MW, molecular weight.

as the regulator of chromatin structure and repressor of gene transcription (13). However, lately HDAC1 has also been implicated in nontranscriptional functions such as DNA repair, splicing, and cell division and has been described as both a positive and a negative regulator of gene expression (13, 24, 43). Some of the genes that are positively regulated by HDAC1 are type I IFNs and ISGs, such as ISG15, ISG54, IFITM1, IFITM2, and viperin (24, 32, 37, 44). Similarly, cellular deacetylase activity also promotes the type I IFN-stimulated expression of ISGs (28–30). In other words, the expression of type I IFNs and ISGs is downregulated in HDAC1-deficient cells and in cells treated with HDAC inhibitors. Therefore, a noticeable decrease in pSTAT1 and IFITM3, ISG15, and viperin levels in TSA-treated IAV-infected cells shown here indicated that class I and class II HDAC activity is an important component of canonical type I IFN-mediated host antiviral response against IAV. Specifically, the decrease or increase in the IAV-induced expression of viperin in HDAC1-depleted or HDAC1-overexpressing cells, respectively, indicated that HDAC1 is a cofactor for the expression of viperin in IAV-infected cells. However, it is unlikely that viperin is the only ISG through which HDAC1 is exerting its anti-IAV function. A direct role of HDAC1 in the expression of other ISGs that inhibit IAV infection remains to be investigated. Further, HDAC1 has been reported to inhibit IAV entry by interfering with host microtubule-mediated endosomal transport, but a direct link between exclusively nuclear HDAC1 and exclusively cytoplasmic microtubule network remains to be elucidated (41).

Previously, a role of HDAC1 (and HDAC2 and -3) has also been studied in the infection of other viruses, especially herpesviruses and HIV-1 that cause both latent and lytic infections (45). Paradoxically, these HDACs play opposing roles during latent and lytic viral infections (46). Because of their role in promoting the compact chromatin organization and repression of transcription, these HDACs promote latency of herpesviruses and HIV-1 and have been the target of HDAC inhibitors to reactivate these viruses for getting rid of the infection (47–50). In contrast, during herpesvirus lytic infections, HDAC1 (and HDAC2) plays an antiviral role by repressing the viral gene transcription and inducing the type I IFN response (44, 49, 51). In gammaherpesvirus-infected primary microphages, HDAC1 (and HDAC2) has been shown to be involved at early steps of the induction of type I IFN response and required for the phosphorylation of interferon regulatory factor 3 (IRF3), the accumulation of phosphorylated IRF3 at the IFN-β promoter, and the subsequent production of type I IFNs (44). The data we have presented here indicate that HDAC1 and deacetylase activity are involved in JAK/STAT pathway induced in IAV-infected cells. However, our data do not demonstrate that HDAC1 or deacetylase activity work upstream and are involved in the production of type I IFNs in IAV-infected cells. It will be interesting to examine the phosphorylation of IRF3 and subsequent production of type I IFNs in HDAC1-depleted and HDAC1-overexpressing cells. The complex IFN signaling pathways represent the first line of host antiviral defense against invading viruses, including IAV. However, like other viruses, IAV has evolved various strategies to subvert IFN signaling to multiply and cause respiratory disease. It has yet to be determined whether HDAC1 plays more of a canonical role or a unique role in the IAV-induced host antiviral response.

With this report, it is clear that at least one member of three main classes of HDACs possesses an anti-IAV function, and HDACs are potentially a novel family of anti-IAV host factors. Recently, we reported that HDAC6, a class II member, inhibits IAV infection (4). Likewise, Koyuncu et al. recently demonstrated that class III HDACs (sirtuins) inhibit IAV infection, too (52). Because of their role in multiple biological processes, HDACs have been the subjects of therapeutic targets for treatment of various human diseases, such as different types of cancers, neurodegen-

erative diseases, and inflammatory disorders (53). The regular emergence of novel, drug-resistant, and zoonotic IAV strains in humans emphasizes the need for the development of an alternative, next-generation anti-IAV strategy. A molecular understanding of IAV and HDACs interplay may lead to the development of such a strategy.

ACKNOWLEDGMENTS

We thank Rory O'Brien, Blair Lawley, Sujan Yellagunda, Sonya Mros, Richard Webby, the Virus Research Unit, and Vernon Ward for technical assistance, materials, and suggestions.

This study was funded by the H. S. and J. C. Anderson Charitable Trust, the Department of Microbiology and Immunology, and the Otago School of Medical Sciences. P.T.N. has been supported by a University of Otago Ph.D. scholarship, and M.H. has been supported by the Health Research Council of New Zealand Emerging Researcher Grant (12/614). The funders had no role in experimental design, data acquisition and interpretation, or the decision to submit the data for publication.

FUNDING INFORMATION

This work, including the efforts of Matloob Husain, was funded by H. S. and J. C. Anderson Trust. This work, including the efforts of Matloob Husain, was funded by Department of Microbiology and Immunology. This work, including the efforts of Matloob Husain, was funded by Te Wahanga Matua Matau Hauora | Otago School of Medical Sciences (OSMS). This work, including the efforts of Prashanth Thevkar Nagesh, was funded by University of Otago (Te Whare Wānanga o Otāgo).

The funders had no role in experimental design, data acquisition and interpretation, or the decision to submit the data for publication.

REFERENCES

1. **Webster RG, Govorkova EA.** 2014. Continuing challenges in influenza. Ann N Y Acad Sci **1323:**115–139. http://dx.doi.org/10.1111/nyas.12462.
2. **Husain M.** 2014. Avian influenza A (H7N9) virus infection in humans: epidemiology, evolution, and pathogenesis. Infect Genet Evol **28:**304–312. http://dx.doi.org/10.1016/j.meegid.2014.10.016.
3. **Duggal NK, Emerman M.** 2012. Evolutionary conflicts between viruses and restriction factors shape immunity. Nat Rev Immunol **12:**687–695. http://dx.doi.org/10.1038/nri3295.
4. **Husain M, Cheung C.** 2014. Histone deacetylase 6 inhibits influenza A virus release by downregulating the trafficking of viral components to the plasma membrane via its substrate acetylated microtubules. J Virol **81:**11229–11239. http://dx.doi.org/10.1128/JVI.00727-14.
5. **Husain M, Harrod KS.** 2011. Enhanced acetylation of alpha-tubulin in influenza A virus-infected epithelial cells. FEBS Lett **585:**128–132. http://dx.doi.org/10.1016/j.febslet.2010.11.023.
6. **Husain M, Harrod KS.** 2009. Influenza A virus-induced caspase-3 cleaves the histone deacetylase 6 in infected epithelial cells. FEBS Lett **583:**2517–2520. http://dx.doi.org/10.1016/j.febslet.2009.07.005.
7. **Haberland M, Montgomery RL, Olson EN.** 2009. The many roles of histone deacetylases in development and physiology: implications for disease and therapy. Nat Rev Genet **10:**32–42. http://dx.doi.org/10.1038/nrg2485.
8. **Allfrey VG, Faulkner R, Mirsky AE.** 1964. Acetylation and methylation of histones and their possible role in the regulation of RNA synthesis. Proc Natl Acad Sci U S A **51:**786–794. http://dx.doi.org/10.1073/pnas.51.5.786.
9. **Galvani A, Thiriet C.** 2015. Nucleosome dancing at the tempo of histone tail acetylation. Genes **6:**607–621. http://dx.doi.org/10.3390/genes6030607.
10. **Choudhary C, Kumar C, Gnad F, Nielsen ML, Rehman M, Walther TC, Olsen JV, Mann M.** 2009. Lysine acetylation targets protein complexes and coregulates major cellular functions. Science **325:**834–840. http://dx.doi.org/10.1126/science.1175371.
11. **Li Y, Shin D, Kwon SH.** 2013. Histone deacetylase 6 plays a role as a distinct regulator of diverse cellular processes. FEBS J **280:**775–7793.
12. **Spiegel S, Milstien S, Grant S.** 2011. Endogenous modulators and pharmacological inhibitors of histone deacetylases in cancer therapy. Oncogene **31:**537–551. http://dx.doi.org/10.1038/onc.2011.267.
13. **Moser MA, Hagelkruys A, Seiser C.** 2013. Transcription and beyond: the role of mammalian class I lysine deacetylases. Chromosoma **2013:**1–12.
14. **Choi J-E, Mostoslavsky R.** 2014. Sirtuins, metabolism, and DNA repair. Curr Opin Genet Dev **26:**24–32. http://dx.doi.org/10.1016/j.gde.2014.05.005.
15. **Emiliani S, Fischle W, Van Lint C, Al-Abed Y, Verdin E.** 1998. Characterization of a human RPD3 ortholog, HDAC3. Proc Natl Acad Sci U S A **95:**2795–2800. http://dx.doi.org/10.1073/pnas.95.6.2795.
16. **Livak KJ, Schmittgen TD.** 2001. Analysis of relative gene expression data using real-time quantitative PCR and the $2^{-\Delta\Delta CT}$ method. Methods **25:**402–408.
17. **van Meerloo J, Kaspers GJ, Cloos J.** 2011. Cell sensitivity assays: the MTT assay. Methods Mol Biol **731:**237–45. http://dx.doi.org/10.1007/978-1-61779-080-5_20.
18. **Walsh D, Mathews MB, Mohr I.** 2013. Tinkering with translation: protein synthesis in virus-infected cells. Cold Spring Harb Perspect Biol **5:**a012351. http://dx.doi.org/10.1101/cshperspect.a012351.
19. **Walsh D, Mohr I.** 2011. Viral subversion of the host protein synthesis machinery. Nat Rev Microbiol **9:**860–875. http://dx.doi.org/10.1038/nrmicro2655.
20. **Wang S, Chi X, Wei H, Chen Y, Chen Z, Huang S, Chen JL.** 2014. Influenza A virus-induced degradation of eukaryotic translation initiation factor 4B contributes to viral replication by suppressing IFITM3 protein expression. J Virol **88:**8375–8385. http://dx.doi.org/10.1128/JVI.00126-14.
21. **Shen S, Zhang P, Lovchik MA, Li Y, Tang L, Chen Z, Zeng R, Ma D, Yuan J, Yu Q.** 2009. Cyclodepsipeptide toxin promotes the degradation of Hsp90 client proteins through chaperone-mediated autophagy. J Cell Biol **185:**629–639. http://dx.doi.org/10.1083/jcb.200810183.
22. **Hassig CA, Tong JK, Fleischer TC, Owa T, Grable PG, Ayer DE, Schreiber SL.** 1998. A role for histone deacetylase activity in HDAC1-mediated transcriptional repression. Proc Natl Acad Sci U S A **95:**3519–3524. http://dx.doi.org/10.1073/pnas.95.7.3519.
23. **Lagger G, O'Carroll D, Rembold M, Khier H, Tischler J, Weitzer G, Schuettengruber B, Hauser C, Brunmeir R, Jenuwein T, Seiser C.** 2002. Essential function of histone deacetylase 1 in proliferation control and CDK inhibitor repression. EMBO J **21:**2672–2681. http://dx.doi.org/10.1093/emboj/21.11.2672.
24. **Zupkovitz G, Tischler J, Posch M, Sadzak I, Ramsauer K, Egger G, Grausenburger R, Schweifer N, Chiocca S, Decker T, Seiser C.** 2006. Negative and positive regulation of gene expression by mouse histone deacetylase 1. Mol Cell Biol **26:**7913–7928. http://dx.doi.org/10.1128/MCB.01220-06.
25. **Dovey OM, Foster CT, Cowley SM.** 2010. Histone deacetylase 1 (HDAC1), but not HDAC2, controls embryonic stem cell differentiation. Proc Natl Acad Sci U S A **107:**8242–8247. http://dx.doi.org/10.1073/pnas.1000478107.
26. **Balasubramanian S, Verner E, Buggy JJ.** 2009. Isoform-specific histone deacetylase inhibitors: the next step? Cancer Lett **280:**211–221. http://dx.doi.org/10.1016/j.canlet.2009.02.013.
27. **Yoshida M, Kijima M, Akita M, Beppu T.** 1990. Potent and specific inhibition of mammalian histone deacetylase both in vivo and in vitro by trichostatin A. J Biol Chem **265:**17174–17179.
28. **Nusinzon I, Horvath CM.** 2003. Interferon-stimulated transcription and innate antiviral immunity require deacetylase activity and histone deacetylase 1. Proc Natl Acad Sci U S A **100:**14742–14747. http://dx.doi.org/10.1073/pnas.2433987100.
29. **Chang HM, Paulson M, Holko M, Rice CM, Williams BR, Marie I, Levy DE.** 2004. Induction of interferon-stimulated gene expression and antiviral responses require protein deacetylase activity. Proc Natl Acad Sci U S A **101:**9578–9583. http://dx.doi.org/10.1073/pnas.0400567101.
30. **Sakamoto S, Potla R, Larner AC.** 2004. Histone deacetylase activity is required to recruit RNA polymerase II to the promoters of selected interferon-stimulated early response genes. J Biol Chem **279:**40362–40367. http://dx.doi.org/10.1074/jbc.M406400200.
31. **Nusinzon I, Horvath CM.** 2006. Positive and negative regulation of the innate antiviral response and beta interferon gene expression by deacetylation. Mol Cell Biol **26:**3106–3113. http://dx.doi.org/10.1128/MCB.26.8.3106-3113.2006.
32. **Xu D, Holko M, Sadler AJ, Scott B, Higashiyama S, Berkofsky-Fessler W, McConnell MJ, Pandolfi PP, Licht JD, Williams BR.** 2009. Promyelocytic leukemia zinc finger protein regulates interferon-mediated innate

immunity. Immunity **30:**802–816. http://dx.doi.org/10.1016/j.immuni.2009.04.013.
33. **García-Sastre, A.** 2011. Induction and evasion of type I interferon responses by influenza viruses. Virus Res **162:**12–18. http://dx.doi.org/10.1016/j.virusres.2011.10.017.
34. **Brass AL, Huang IC, Benita Y, John SP, Krishnan MN, Feeley EM, Ryan BJ, Weyer JL, van der Weyden L, Fikrig E, Adams DJ, Xavier RJ, Farzan M, Elledge SJ.** 2009. The IFITM proteins mediate cellular resistance to influenza A H1N1 virus, West Nile virus, and dengue virus. Cell **139:**1243–1254. http://dx.doi.org/10.1016/j.cell.2009.12.017.
35. **Lenschow DJ, Lai C, Frias-Staheli N, Giannakopoulos NV, Lutz A, Wolff T, Osiak A, Levine B, Schmidt RE, García-Sastre A, Leib DA, Pekosz A, Knobeloch KP, Horak I, Virgin HW, IV.** 2007. IFN-stimulated gene 15 functions as a critical antiviral molecule against influenza, herpes, and Sindbis viruses. Proc Natl Acad Sci U S A **104:**1371–1376. http://dx.doi.org/10.1073/pnas.0607038104.
36. **Wang X, Hinson ER, Cresswell P.** 2007. The interferon-inducible protein viperin inhibits influenza virus release by perturbing lipid rafts. Cell Host Microbe **2:**96–105. http://dx.doi.org/10.1016/j.chom.2007.06.009.
37. **Kim YE, Ahn JH.** 2015. Positive role of promyelocytic leukemia protein in type I interferon response and its regulation by human cytomegalovirus. PLoS Pathog **11:**e1004785. http://dx.doi.org/10.1371/journal.ppat.1004785.
38. **Buggele WA, Krause KE, Horvath CM.** 2013. Small RNA profiling of influenza A virus-infected cells identifies miR-449b as a regulator of histone deacetylase 1 and interferon beta. PLoS One **8:**e76560. http://dx.doi.org/10.1371/journal.pone.0076560.
39. **Gaughan L, Logan IR, Neal DE, Robson CN.** 2005. Regulation of androgen receptor and histone deacetylase 1 by Mdm2-mediated ubiquitylation. Nucleic Acids Res **33:**13–26. http://dx.doi.org/10.1093/nar/gki141.
40. **Kwon DH, Eom GH, Ko JH, Shin S, Joung H, Choe N, Nam YS, Min HK, Kook T, Yoon S, Kang W, Kim YS, Kim HS, Choi H, Koh JT, Kim N, Ahn Y, Cho HJ, Lee IK, Park DH, Suk K, Seo SB, Wissing ER, Mendrysa SM, Nam KI, Kook H.** 2016. MDM2 E3 ligase-mediated ubiquitination and degradation of HDAC1 in vascular calcification. Nat Commun **7:**10492. http://dx.doi.org/10.1038/ncomms10492.
41. **Yamauchi Y, Boukari H, Banerjee I, Sbalzarini IF, Horvath P, Helenius A.** 2011. Histone deacetylase 8 is required for centrosome cohesion and influenza A virus entry. PLoS Pathog **7:**e1002316. http://dx.doi.org/10.1371/journal.ppat.1002316.
42. **Taunton J, Hassig CA, Schreiber SL.** 1996. A mammalian histone deacetylase related to the yeast transcriptional regulator Rpd3p. Science **272:**408–411. http://dx.doi.org/10.1126/science.272.5260.408.
43. **Wang Z, Zang C, Cui K, Schones DE, Barski A, Peng W, Zhao K.** 2009. Genome-wide mapping of HATs and HDACs reveals distinct functions in active and inactive genes. Cell **138:**1019–1031. http://dx.doi.org/10.1016/j.cell.2009.06.049.
44. **Mounce BC, Mboko WP, Kanack AJ, Tarakanova VL.** 2014. Primary macrophages rely on histone deacetylase 1 and 2 expression to induce type I interferon in response to gammaherpesvirus infection. J Virol **88:**2268–2278. http://dx.doi.org/10.1128/JVI.03278-13.
45. **Herbein G, Wendling D.** 2010. Histone deacetylases in viral infections. Clin Epigenet **1:**13–24. http://dx.doi.org/10.1007/s13148-010-0003-5.
46. **Roizman B.** 2011. The checkpoints of viral gene expression in productive and latent infection: the role of the HDAC/CoREST/LSD1/REST repressor complex. J Virol **85:**7474–7482. http://dx.doi.org/10.1128/JVI.00180-11.
47. **Archin NM, Espeseth A, Parker D, Cheema M, Hazuda D, Margolis DM.** 2009. Expression of latent HIV induced by the potent HDAC inhibitor suberoylanilide hydroxamic acid. AIDS Res Hum Retroviruses **25:**207–212. http://dx.doi.org/10.1089/aid.2008.0191.
48. **Manson McManamy ME, Hakre S, Verdin EM, Margolis DM.** 2014. Therapy for latent HIV-1 infection: the role of histone deacetylase inhibitors. Antivir Chem Chemother **23:**145–149. http://dx.doi.org/10.3851/IMP2551.
49. **Guise AJ, Budayeva HG, Diner BA, Cristea IM.** 2013. Histone deacetylases in herpesvirus replication and virus-stimulated host defense. Viruses **5:**1607–1632. http://dx.doi.org/10.3390/v5071607.
50. **Shin HJ, DeCotiis J, Giron M, Palmeri D, Lukac DM.** 2014. Histone deacetylase classes I and II regulate Kaposi's sarcoma-associated herpesvirus reactivation. J Virol **88:**1281–1292. http://dx.doi.org/10.1128/JVI.02665-13.
51. **Mounce BC, Mboko WP, Bigley TM, Terhune SS, Tarakanova VL.** 2013. A conserved gammaherpesvirus protein kinase targets histone deacetylases 1 and 2 to facilitate viral replication in primary macrophages. J Virol **87:**7314–7325. http://dx.doi.org/10.1128/JVI.02713-12.
52. **Koyuncu E, Budayeva HG, Miteva YV, Ricci DP, Silhavy TJ, Shenk T, Cristea IM.** 2014. Sirtuins are evolutionarily conserved viral restriction factors. mBio **5:**e02249–14. http://dx.doi.org/10.1128/mBio.02249-14.
53. **Micelli C, Rastelli G.** 2015. Histone deacetylases: structural determinants of inhibitor selectivity. Drug Discov Today **20:**718–735. http://dx.doi.org/10.1016/j.drudis.2015.01.007.